Eur. Phys. J. D **62**, 433–437 (2011)
DOI: 10.1140/epjd/e2011-20036-1

THE EUROPEAN PHYSICAL JOURNAL D

Regular Article

Experimental generation of optical non-classical states of light with 1.34 μm wavelength

F.Y. Hou, L. Yu, X.J. Jia[a], Y.H. Zheng, C.D. Xie, and K.C. Peng

State Key Laboratory of Quantum Optics and Quantum Optics Devices, Institute of Opto-Electronics, Shanxi University, Taiyuan, 030006, P.R. China

Received 22 October 2010 / Received in final form 17 February 2011
Published online 25 March 2011 –

Abstract. We report the experimental generation of the optical non-classical states with 1.34 μm wavelength which is close to one of the fiber telecommunication windows (1.31 μm). The single-mode amplitude squeezed states with quantum fluctuation of 2.3 ± 0.1 dB below the shot noise limit (SNL) and the entangled states with quantum correlation of 1.1 ± 0.1 dB below the SNL are produced by an optical parametric amplifier with a type-I phase-matched PPKTP crystal and a pair of properly oriented type-II phase-matched KTP crystals, respectively.

1 Introduction

The continuous variable (CV) non-classical state of light have been extensively studied [1]. It has been theoretically and experimentally demonstrated that squeezed states and entangled states of optical modes can be used for implementing quantum measurements with precisions higher than the shot noise limit (SNL) [2,3] and novel quantum communications which can not be performed in the frame of classical physics, such as quantum teleportation [4] and quantum dense coding [5,6]. In 1985, the first observation of the squeezed states of light at 0.59 μm wavelength was experimentally achieved through the degenerate four-wave-mixing in Na vapor by Slusher et al. [7]. Successively, J. Kimble's group obtained the squeezed state of light at 1.06 μm wavelength with much higher squeezing degree of 4.3 dB by means of degenerate parametric down conversion in an optical cavity [8]. Based on nondegenerate four-wave mixing in a hot vapor, the bright twin beams at 0.79 μm wavelength which display a quantum noise reduction in the intensity difference of more than 8 dB was obtained by Lett's group [9]. Till now, the single-mode squeezed light beams of ∼9 dB at 0.86 μm wavelength and 11.5 dB at 1.06 μm wavelength were generated from a degenerate optical parametric amplifier (OPA) with a PPKTP (periodically poled KTiOPO4) crystal and a monolithic degenerate OPA made by MgO: LiNbO3 crystal, respectively [10,11]. At the beginning of 1990s, Kimble's group experimentally generated a pair of CV entangled optical beams at 1.08 μm wavelength by type-II down-conversion in a subthreshold non-degenerate OPA and demonstrated the Einstein-Podolsky-Rosen (EPR) paradox firstly in CV regime [12]. The entangled beams at 1.06 μm wavelength are also generated from the interference of two amplitude squeezed beams by Bowen et al. [13]. The first measurement of squeezed-state entanglement between the twin beams at 1.06 μm wavelength produced by an optical parametric oscillator operating above threshold was finished by Villar et al. [14]. Experimental generation of entangled optical beams with 1.06 μm wavelength from a type-II frequency-degenerate optical parametric oscillator below threshold with a quarter-wave plate inserted inside the cavity was achieved by Fabre's group [15]. Later, CV entanglement with 1.06 μm wavelength between the bright beams emitted by an optical parametric oscillator above threshold was also observed by several groups [16,17]. The experimental observation of bright EPR beams with 1.06 μm wavelength produced by a type-II optical parametric oscillator operating above threshold at frequency degeneracy was achieved by Keller et al. in 2008 [18]. CV optical entangled states at 1.08 μm wavelength with amplitude and phase quadrature quantum correlations was enhanced to ∼6 dB recently [19]. However, the transparency windows of the silica-based commercial optical fibers are around 1.55 μm or 1.31 μm wavelength. As well known, any loss will severely destroy the squeezing and entanglement of light. For example, after a squeezed light with the same squeezing of 5.0 dB and the different wavelength at 1.06 μm, 1.31 μm and 1.55 μm respectively transmits 5 km in a normal fiber, the retained squeezing will be 1.0 dB, 2.6 dB and 3.4 dB respectively. That is because the transmission losses in the optical fiber for the light at 1.06 μm, 1.31 μm and 1.55 μm are 1.0 dB/km, 0.35 dB/km and 0.20 dB/km, respectively (see the conclusion of the context and reference [20] for details). Thus to develop the practical quantum telecommunication, we have to pay attention in the investigation of non-classical

[a] e-mail: jiaxj@sxu.edu.cn

light generation at the two window wavelengths firstly. Recent years, the squeezed states and entangled states of light around 1.55 μm have been experimentally obtained [21–27]. Although the absorption losses in fibers for 1.55 μm wavelength is less than that for 1.31 μm, the phase diffusion effect of 1.31 μm light is much smaller than that of 1.55 μm light. The phase diffusion of light will strongly increase the phase noise and decrease the phase correlation of optical fields. In quantum information system sometimes the requirement for the phase noise is specially strict, thus it is also necessary to prepare the nonclassical light around 1.31 μm wavelength besides 1.55 μm. To the best of our knowledges, the study on the generation system of the squeezed state and the entangled state of light around 1.31 μm has not been reported, so far.

In this paper, we present the design of a single-frequency all-solid-state Nd:YVO_4 laser with 1.34 μm output wavelength, as well as the experimental systems and results for the non-classical light generation at 1.34 μm. The squeezed states and the entangled states of light are generated through a frequency-down conversion process in an OPA pumped by the home-made frequency-doubled and single-frequency Nd:YVO_4 laser system operating at 1.34 μm wavelength. The single-mode squeezed states with the amplitude quadrature squeezing of 2.3 ± 0.1 dB below the SNL and the entangled states with the amplitude and the phase quantum correlations of 1.1 ± 0.1 dB below the corresponding SNL at 1.34 μm are produced directly by the OPA with a type-I phase-matched PPKTP crystal and a pair of type-II phase-matched bulk KTP crystals with their optical axes symmetrically crossed, respectively.

2 Experimental setup

Not like popular 1.06 μm laser there is no any commercial single-frequency continuous-wave (CW) laser with required powers for pumping OPA to produce ∼1.3 μm nonclassical light. So the first task is to design and build an appropriate pump source of the OPA. Besides the normal 1.06 μm laser transition there is also another possible laser transition at 1.34 μm in Nd:YVO_4 crystal [28,29]. However for usually used Nd:YVO_4 laser crystal, the stimulated emission cross section at 1.34 μm is smaller than that at 1.06 μm and the thermal effect induced by laser in the crystal for 1.34 μm is stronger than that for 1.06 μm since there is lager energy difference between the pump photons of the laser diode (LD) at 0.80 μm and the photons at 1.34 μm than that at 1.06 μm. The two negative factors have to be taken care in the design of 1.34 μm Nd:YVO_4 laser. By employing highly selective dielectrically coated mirrors with high transmission at 1.06 μm to be the cavity mirrors of the laser resonator the optimal oscillation condition for 1.34 μm is reached and the oscillation for 1.06 μm is suppressed. To mitigate the thermal effect a low-doped composite Nd:YVO_4 crystal with $3\times3\times6$ mm^3 YVO_4 and $3 \times 3 \times 7$ mm^3 Nd:YVO_4 serves as the laser crystal, the two end-faces of which are coated with antireflective films at 0.80 μm, 1.06 μm and 1.34 μm. The laser resonator is in the bow-tie ring configuration consisting of four cavity mirrors. A fiber coupled LD (JOLD-30-FC-14-808 from JENOPTIK) is used for the pump source of the Nd:YVO4 laser. A Faraday rotator and a half wave plate at 1.34 μm are placed in the cavity to ensure the unidirectional operation of the laser. When the pump power of LD is 18 W, the single-frequency laser of 1.8 W at 1.34 μm was obtained. The intensity fluctuation of the output laser is less than ±0.5% in an hour and its frequency shift in a minute is less than ±2 MHz under the condition of free running.

The second-harmonic-generator (SHG) with F-P configuration consists of two spherical mirrors with 50 mm radius of curvature. The input mirror (M1) has a reflectivity of 97% at 1.34 μm and is high reflective at the second-harmonic-wave of 0.67 μm. A piezo-transducer (PZT) driven mirror (M2) with high reflection at 1.34 μm and high transmission at 0.67 μm is employed as the output coupler. A nonlinear crystal LBO of $3 \times 3 \times 20$ mm^3 dimension with the dual-band antireflection of 1.34 μm and 0.67 μm at both end-faces is placed in the middle of the F-P cavity of 103 mm-long to implement the frequency up-conversion of the fundamental wave at 1.34 μm. When the pump power at 1.34 μm is 1.14 W, the second-harmonic-wave of 580 mW at 0.67 μm is obtained with the frequency-doubling efficiency of 50.9%.

The OPA is also in the F-P configuration consisting of two spherical mirrors with 50 mm radius of curvature. The length of the F-P cavity is 103 mm and the nonlinear optical element is placed at the middle of the cavity for achieving the frequency down conversion of the pump field at 0.67 μm to generate the required nonclassical states of light at 1.34 μm. The input mirror (M3) of the OPA is coated with the high reflectivity at 1.34 μm and the high transmission at 0.67 μm. The output mirror (M4) is coated with the high reflectivity at 0.67 μm and the transmission of 3.0% at 1.34 μm to be used for the output coupler of the generated nonclassical states of light. The M4 is mounted on a PZT to implement the cavity scanning or locking actively as needed. A type-I phase matching PPKTP crystal with the dimension of $1 \times 3 \times 15$ mm^3 and the poled period of 52 μm serves as the nonlinear optical element in the OPA for the generation of the single-mode squeezed states at 1.34 μm. To generate the EPR entangled states the PPKTP is substituted by a pair of type-II phase-matching bulk crystals [30–32] (the dimension of each crystal is $3 \times 3 \times 10$ mm^3). For reducing the transmission losses all end-faces of these crystals are coated with antireflectivity at both 1.34 μm and 0.67 μm. The PPKTP (a pair of KTP) is put in a specially designed temperature controller to control the temperature of the crystal at its optimal phase-matching point around 170 °C (25 °C) with the accuracy of 0.005 °C. The finesse of the OPA with PPKTP (a pair of KTP) is 157 (136).

The standard balanced homodyne detector (BHD) consisting of a 50/50-beamsplitter and a pair of balanced photodiodes (ETX500 InGaAs photodiode from JDSU) with the quantum efficiency of 93% is used for the detection system to measure the quantum fluctuation of the quadrature components of electromagnetic fields. When

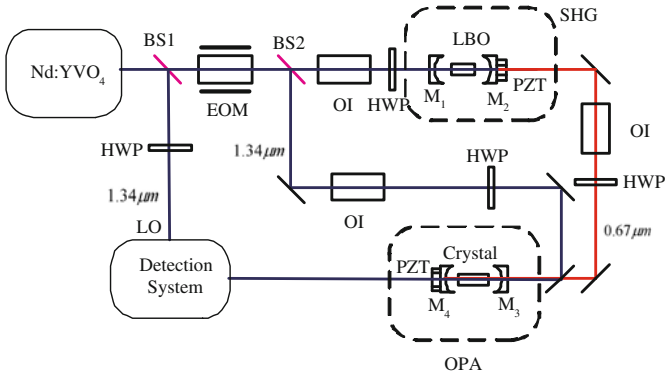

Fig. 1. (Color online) Experimental setup. Nd:YVO_4, laser source; SHG, second harmonic generator; OPA, optical parametric amplifier; EOM, electro-optical modulator; OI, optical isolators; HWP, half wave plate; BS1-2, different beam splitter; M1-4, different mirrors; PZT, piezo electric transducer; crystal, a PPKTP for the generation of the amplitude squeezed states of light and a pair of KTP for the generation of EPR entangled beams.

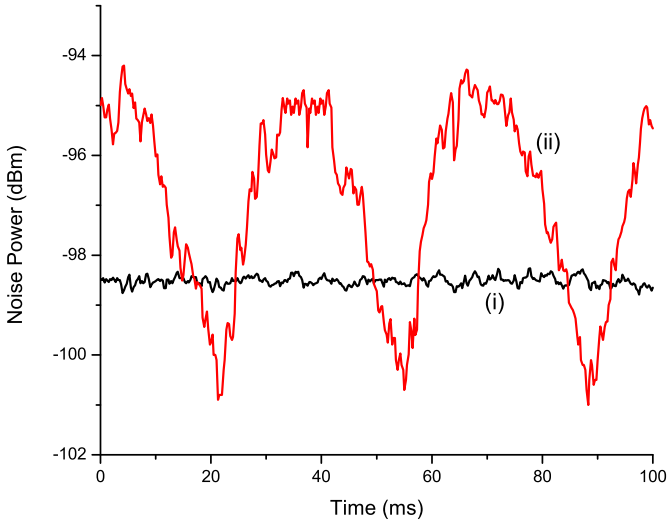

Fig. 2. (Color online) The noise powers of the amplitude squeezed light at a sideband of 3.0 MHz. Trace (i): SNL; trace (ii): the noise power recorded by sweeping the LO phase. The measurement parameters of SA: resolution band width is 30 kHz; video band width is 100 Hz.

the single-mode amplitude squeezed states is detected a local oscillation (LO) light from the Nd:YVO_4 laser is required as usual. When the EPR entangled states produced from the OPA operating at anti-amplification is detected, the LO light is not needed. In this case the two entangled beams are combined on the 50/50-beamsplitter and then the sum (difference) of the photocurrents detected by the two photodiodes directly represents the quantum correlation of amplitude (phase) quadratures between two EPR beams. This self-homodyne detection system also was named the direct Bell-state detector [33].

The schematic of the experimental system is shown in Figure 1. The laser from the Nd:YVO_4 at 1.34 μm is splitted by a beam-splitter (BS1) in two parts, the small one of which (∼20 mW) serves as the local oscillator (LO) for the detection of the single-mode squeezing. The remaining large part is modulated by an electro-optics modulator (EOM) with a modulation frequency of ∼70 MHz firstly. The aim of the modulation is for locking the SHG and the OPA to resonate with the pump field and the injected signal field at 1.34 μm, respectively. The modulated laser is separated again by BS2, the smaller part of which (∼10 mW) is sent into the OPA to be the injected signal and the larger part is sent into the SHG to be the pump laser. The second-harmonic-wave at 0.67 μm produced by the SHG is sent into the OPA to be the pump light for achieving the non-classical light generation via an intracavity frequency-down conversion process. The optical isolators (OI) are placed on the optical paths to eliminate the optical feedback of the cavity mirrors and the half-wave plates are used for the polarization alignment of the pump (signal) light beams with respect to the optical axis of the nonlinear crystals inside the SHG and the OPA. The OPA is operated below the oscillation threshold and the relative phase between its pump field at 0.67 μm and the injected signal field at 1.34 μm are locked at $(2n+1)\pi$ (n is the integer), that is to force the OPA to operate at anti-amplification [6]. In this case, the squeezed states with the squeezed amplitude-quadrature component and the anti-squeezed phase-quadrature component [34] as well as the entangled states with the amplitude-quadrature anti-correlation and the phase-quadrature correlation [6] are generated by the OPA with the type-I PPKTP and a pair of type-II KTP crystals, respectively.

3 Experimental results

For the generation of single-mode squeezed state of light, we put the PPKTP crystal inside the OPA cavity. The measured finesse of the OPA is 157, and thus the corresponding extra intra-cavity total losses is 1.0%, which contain 0.8% loss in the PPKTP crystal and 0.2% on the two mirrors of the cavity. Figure 2 shows the measured noise power at a sideband of 3.0 MHz for the single-mode squeezed state of light generated by the OPA while the phase of the LO beam is scanned. Trace (i) represents the SNL measured by blocking the output of the OPA and only the LO beam entering the BHD detection system. The SNL level is also calibrated by a thermal white light source with the same power [35]. Trace (ii) is the measured phase dependence of the quantum noise in the squeezed state of light. The maximum squeezing of 2.3 ± 0.1 dB below the SNL is achieved. After considering the detection efficiency of photodiode (92%) and the imperfect mode matching between LO beam and the squeezed states of light (98%), the the actual squeezing should be 2.6 dB below the SNL. The intensity of the squeezed light is about 32 μW. The measurement parameters of the used spectral analyzer (SA) are: the central frequency – 3.0 MHz, the resolution bandwidth – 30 kHz and the video bandwidth – 100 Hz.

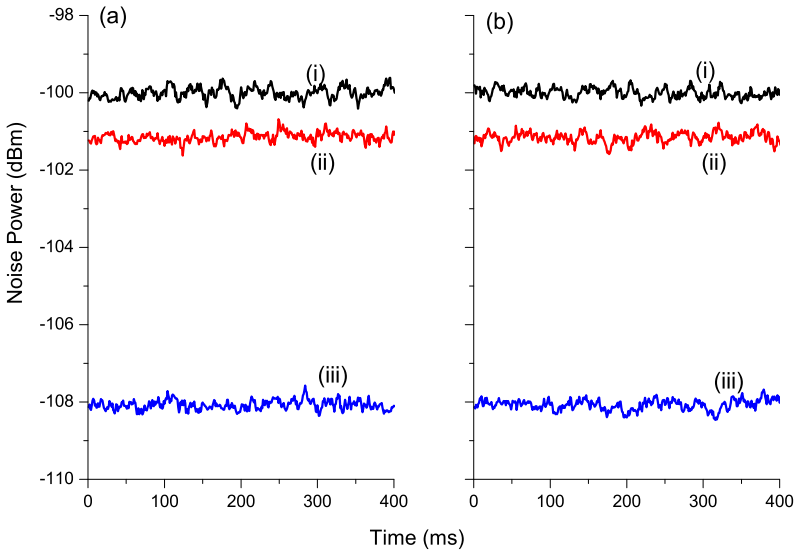

Fig. 3. (Color online) The noise powers of the correlation variances of the output EPR entangled beams from OPA operated at de-amplification at a sideband of 3.0 MHz: (a) for amplitude sum; (b) for phase difference. Trace (i): SNL; trace (ii): correlation variances; trace (iii): ENL. The measurement parameters of SA: resolution band width is 30 kHz; video band width is 100 Hz.

Using the OPA with a pair of type-II phase-matched bulk KTP crystals with their optical axes symmetrically crossed [30–32], a pair of EPR entangled optical beams of 28 μW with orthogonal polarizations and the identical frequency at 1.34 μm are obtained under the pump power of 200 mW. In this case, the finesse of the OPA was decreased to 136, due to the extra loss of the OPA was increased to about 1.6%. The output beams of OPA are separated by a polarizing-beam-splitter and then is detected by the Bell-state direct detection system [33] while the LO beam is blocked. The trace (ii) in Figures 3a and 3b are the recorded correlation variances of the amplitude sum $\langle\delta^2(X_a + X_b)\rangle$ and the phase difference $\langle\delta^2(Y_a - Y_b)\rangle$ between the two beams, respectively, where $X_{a(b)}$, $Y_{a(b)}$ are the amplitude and phase quadratures of the output beam $a(b)$. Both of them are 1.1 ± 0.1 dB below the corresponding SNL (trace (i)) and the generated bright EPR entangled beams satisfy the inseparable criteria of quantum states given in reference [36,37]: $\langle\delta^2(X_a+X_b)\rangle+\langle\delta^2(Y_a-Y_b)\rangle = 1.55 < 2$. The trace (iii) in Figures 3a and 3b are the corresponding electric noise level (ENL) both of which are 8.0 dB below the corresponding SNL. After considering the influence of electronics noise, the detection efficiency of photodiode and the imperfect mode matching, the the actual squeezing should be 1.4 dB below the SNL.

4 Discussion and conclusion

Although the obtained squeezing and the entanglement degrees at 1.34 μm wavelength in the present experiments are not high enough, its much lower transmission losses than that of other wavelengths will make it being useful in the telecommunication in fibers. So far, the high squeezing up to 11.5 dB at 1.06 μm wavelength is available [11]. However, due to that the transmission losses of 1.06 μm and 1.34 μm wavelength in fibers are 1.0 dB/km and 0.4 dB/km respectively, after a fiber transmission of 5 km, the transmission efficiency of 1.06 μm and 1.34 μm wavelength are 0.10 and 0.42 respectively, the squeezing of 1.06 μm light reduces from 11.5 dB (the corresponding squeezing level is $10^{(-11.5/10)} = 0.071$) to 0.4 dB (the corresponding squeezing level is $0.071 \times 0.10 + (1 - 0.10) = 0.907$) and for 1.34 μm light the squeezing only reduces from 2.3 dB (the corresponding squeezing level is 0.59) to 0.8 dB (the corresponding squeezing level is $0.59 \times 0.42 + (1 - 0.42) = 0.8278$) (see Eq. (9.3.2) of Ref. [20] for details). The advantage of 1.34 μm squeezed state of light is obvious in the long distance fiber communication.

The transmission loss of the PPKTP used in our experiment is 0.8% due to the absorption of the crystal and the imperfect coating at two end-faces. If the losses in the crystal can be reduced to 0.4% and the transmission of the OPA output coupler is increased to 5.0% to make the escape efficiency of the optical cavity be improved from 0.75 to 0.90, the squeezing of the 1.34 μm will possibly increase to 6 dB using the same experimental system (see Eq. (2) in Ref. [10]). On the other side, if the pair of type-II bulk KTP crystals can be replaced by a type-II PPKTP with much lower losses the obtained entanglement using the presented scheme will be significantly increased. Such as if the losses in the crystals decrease from 1.4% to 0.4% and the nonlinear coefficient keeps unchanging, the escape efficiency will be improved from 0.65 to 0.83, and the entanglement will increase from 1.1 dB to 3.8 dB.

For the conclusion, we experimentally generate the squeezed states and the entangled states of light with 1.34 μm wavelength close to a transparency window of telecommunication. The presented system has potential application in the future long distance quantum information with continuous variables.

This research was supported by Natural Science Foundation of China (Grants Nos. 60736040, 61008001 and 11074157), NSFC Project for Excellent Research Team (Grant No. 60821004), National Basic Research Program of China (Grant No. 2010CB923103).

References

1. S.L. Braunstein, P. van Loock, Rev. Mod. Phys. **77**, 513 (2005)
2. M. Xiao, L.-A. Wu , H.J. Kimble, Phys. Rev. Lett. **59**, 278 (1987)
3. K. Goda, O. Miyakawa, E.E. Mikhailov, S. Saraf, R. Adhikari, K. McKenzie, R. Ward, S. Vass, A.J. Weinstein, N. Mavalvala, Nature Phys. **4**, 472 (2008)
4. A. Furusawa, J.L. Sorensen, S.L. Braunstein, C.A. Fuchs, H.J. Kimble, E.S. Polzik, Science **282**, 706 (1998)
5. S.F. Pereira, Z.Y. Ou, H.J. Kimble, Phys. Rev. A **62**, 042311 (2000)
6. X.Y. Li, Q. Pan, J.T. Jing, J. Zhang, C.D. Xie, K.C. Peng, Phys. Rev. Lett. **88**, 047904 (2002)
7. R.E. Slusher, L.W. Hollberg, B. Yurke, J.C. Mertz, J.F. Valley, Phys. Rev. Lett. **55**, 2409 (1985)
8. Ling-An Wu, H.J. Kimble, J.L. Hall, Huifa Wu, Phys. Rev. Lett. **57**, 2520 (1986)
9. C.F. McCormick, A.M. Marino, V. Boyer, P.D. Lett, Phys. Rev. A **78**, 043816 (2008)
10. Y. Takeno, M. Yukawa, H. Yonezawa, A. Furusawa, Opt. Express **15**, 4321 (2007)
11. M. Mehmet, H. Vahlbruch, N. Lastzka, K. Danzmann, R. Schnabel, Phys. Rev. A **81**, 013814 (2010)
12. Z.Y. Ou, S.F. Pereira, H.J. Kimble, K.C. Peng, Phys. Rev. Lett. **68**, 3663 (1992)
13. W.P. Bowen, R. Schnabel, P.K. Lam, T.C. Ralph, Phys. Rev. Lett. **90**, 043601 (2003)
14. A.S. Villar, L.S. Cruz, K.N. Cassemiro, M. Martinelli, P. Nussenzveig, Phys. Rev. Lett. **95**, 243603 (2005)
15. J. Laurat, T. Coudreau, G. Keller, N. Treps, C. Fabre, Phys. Rev. A **71**, 022313 (2005)
16. X.L. Su, A.H. Tan, X.J. Jia, Q. Pan, C.D. Xie, K.C. Peng, Opt. Lett. **31**, 1133 (2006)
17. J.T. Jing, S. Feng, R. Bloomer, O. Pfister, Phys. Rev. A **74**, 041804 (2006)
18. G. Keller, V. D'Auria, N. Treps, T. Coudreau, J. Laurat, C. Fabre, Opt. Express **16**, 9351 (2008)
19. Y. Wang, H. Shen, X.L. Jin, X.L. Su, C.D. Xie, K.C. Peng, Opt. Express **18**, 6149 (2010)
20. H.A. Bachor, T.C. Ralph, *A Guide to Experiments in Quantum Optics* (Wiley-VCH Verlag GmbH & Co. KGaA, 2004), p. 258
21. X. Li, P.L. Voss, J.E. Sharping, P. Kumar, Phys. Rev. Lett. **94**, 053601 (2005)
22. Ch. Silberhorn, P.K. Lam, O. Weiß, F. König, N. Korolkova, G. Leuchs, Phys. Rev. Lett. **86**, 4267 (2001)
23. N. Nishizawa, K. Sone, J. Higuchi, M. Mori, K. Yamane, T. Goto, Jpn J. Appl. Phys. **41**, L130 (2002)
24. Y. Eto, T. Tajima, Y. Zhang, T. Hirano, Opt. Lett. **32**, 1698 (2007)
25. J.X. Feng, X.T. Tian, Y.M. Li, K.S. Zhang, Appl. Phys. Lett. **92**, 221102 (2008)
26. R. Dong, J. Heersink, J. Corney, P. Drummond, U. Andersen, G. Leuchs, Opt. Lett. **33**, 116 (2008)
27. M. Mehmet, S. Steinlechner, T. Eberle, H. Vahlbruch, A. Thūring, K. Danzmann, R. Schnabel, Opt. Lett. **34**, 1060 (2009)
28. A. Agnesi, G.C. Reali, P.G. Gobbi, IEEE J. Quantum Electron. **34**, 1297 (1998)
29. D.X. Chang, X. Liu, Y. Wang, X.J. Jia, K.C. Peng, Chin. J. Lasers **35**, 323 (2008)
30. J.R. Gao, H. Wang, M.Q. Huang, C.D. Xie, K.C. Peng, Appl. Opt. **34**, 1519 (1995)
31. L.K. Samanta, T. Yanagawa, Y. Yamamoto, Opt. Commun. **76**, 250 (1990)
32. I.N. Agafonov, M.V. Chekhova, G. Leuchs, Phys. Rev. A **82**, 011801 (2010)
33. J. Zhang, K.C. Peng, Phys. Rev. A **62**, 064302 (2000)
34. W.P. Bowen, N. Treps, B.C. Buchler, R. Schnabel, T.C. Ralph, H.A. Bachor, T. Symul, P.K. Lam, Phys. Rev. A **67**, 032302 (2003)
35. H.A. Bachor, T.C. Ralph, *A Guide to Experiments in Quantum Optics* (Wiley-VCH Verlag GmbH & Co. KGaA, 2004), p. 203
36. M.D. Reid, Phys. Rev. A **40**, 913 (1989)
37. Lu-Ming Duan, G. Giedke, J.I. Cirac, P. Zoller, Phys. Rev. Lett. **84**, 2722 (2000)